Optical Engineering

SPIEDigitalLibrary.org/oe

Experimental study on the multisoliton pattern formation in an erbium-doped fiber laser passively mode-locked by graphene saturable absorber

Qi Feng
Yu Chen
Chujun Zhao
Ying Li
Jianguo Wen
Han Zhang

Experimental study on the multisoliton pattern formation in an erbium-doped fiber laser passively mode-locked by graphene saturable absorber

Qi Feng
Hunan University
Key Laboratory for Micro-/Nano-Optoelectronic Devices of Ministry of Education
College of Information Science and Engineering
Changsha 410082, China

Yu Chen
Chujun Zhao
Ying Li
Hunan University
Key Laboratory for Micro-/Nano-Optoelectronic Devices of Ministry of Education
College of Physics and Microelectronic Science
Changsha 410082, China

Jianguo Wen
Hunan University
Key Laboratory for Micro-/Nano-Optoelectronic Devices of Ministry of Education
College of Information Science and Engineering
Changsha 410082, China
E-mail: jgwen911@126.com

Han Zhang
Hunan University
Key Laboratory for Micro-/Nano-Optoelectronic Devices of Ministry of Education
College of Physics and Microelectronic Science
Changsha 410082, China

Abstract. We demonstrate an erbium-doped fiber laser passively mode-locked by few layers of graphene prepared by the mechanical exfoliation of the high oriented pyrolytic graphite through the Scotch-tape method. This all-fiber ring cavity delivered a pulse train with a repetition rate of 1.646 MHz and pulse duration of 1.656 ps. By continuously adjusting the laser cavity parameters, one can observe various soliton patterns, such as ordered-, chaotic-, bunched-, and harmonic-multisoliton state. This evidenced that a mode-locked fiber laser based on graphene saturable absorber indeed provided a well-controlled nonlinear optics platform for soliton dynamics study. [DOI: 10.1117/1.OE.52.4.044201]

Subject terms: multisoliton; mode-locked fiber laser; graphene saturable absorber.

Paper 121857 received Dec. 21, 2012; revised manuscript received Mar. 6, 2013; accepted for publication Mar. 18, 2013; published online Apr. 15, 2013.

1 Introduction

Graphene, a single two-dimensional atomic layer of carbon atoms arranged in a benzene-ring-like structure, was isolated for the first time by Novoselov et al.[1] Subsequently, graphene attracted much attention due to its distinctive electronic and optical properties that originate from its Dirac energy band structure. Graphene saturable absorber (SA) devices possess some unique optic merits, such as low saturable intensity, wideband tunability, and high modulation depth.[2–5] Since the first successful demonstration of graphene SA in 2009,[2] graphene SA is widely recognized as the next-generation passive mode locker that can replace conventional mode locking technique. Different kinds of fiber laser with erbium-,[6–14] ytterbium-,[15–17] thulium-doped fibers,[18,19] and solid-state laser with neodymium-,[20,21] ytterbium-,[22] thulium-doped crystal,[23] have been demonstrated based on the graphene SAs.

Besides saturable absorption, Hendry et al. demonstrated that graphene shows an exceptionally high nonlinear optics response.[24] Zhang et al. experimentally verified that besides the well-known saturable absorption effect, graphene also possesses a large nonlinear refractive index of $n_2 = 10^{-7}$ cm^{2}W^{-1} (eight orders of magnitude larger than silica) and also distinguished the real and imaginary part of the complex nonlinear refractive index of graphene.[25] A very interesting question arises that the nonlinear Kerr effect in graphene may impact the formation of multisoliton pulses. Moreover, mode-locking fiber laser is normally considered as an ideal test bed for soliton dynamics study. The marriage between the unique nonlinear optics property in graphene and nonlinear laser cavity dynamics may lead to new optical physics. Worthy of mentioning are that, with graphene SA, Meng et al. investigated the multiple-soliton formation;[26] Sobon et al. demonstrated a very high-repetition-rate (21st, 2.22 GHz) of harmonic mode-locking with subpicosecond pulse duration and over 40 dB super-mode suppression;[27] and a pulse train with a repetition rate of 502.84 MHz, 50 dB super-mode suppression and 67 dB signal-to-noise ratio was reported by Fu et al.[28] In this paper, a graphene SA device, which was fabricated through the mechanical exfoliation of graphite, was used to produce various different

0091-3286/2013/$25.00 © 2013 SPIE

soliton operation states. This systematic experimental study clearly shows that graphene SA prepared by mechanical exfoliation method could operate as an effective SA for soliton dynamics study in a fiber laser platform.

2 Experimental Section

2.1 *Graphene Preparation and Characterization*

Graphene-based SAs can be prepared by chemical methods, including chemical vapor deposition,[29] epitaxial growth,[30] and reduction of exfoliated graphite oxide nano-platelets.[31] However, additional chemical synthesis tools and transfer process steps are required for these chemical methods. In our experiments, another efficient physical method, which is based on mechanical exfoliation of graphene from pure graphite,[32,33] also known as "Scotch-tape method," was used for the fabrication of graphene SAs, as shown in Fig. 1. Starting from the commercially available highly oriented pyrolytic graphite (HOPG) (SPI Company), this HOPG sample was moderately peeled through a Scotch tape in order to obtain graphite flakes. Then the flakes adhered on the Scotch tape were pressed repeatedly to make graphite become thinner, finally leading to the formation of multilayer

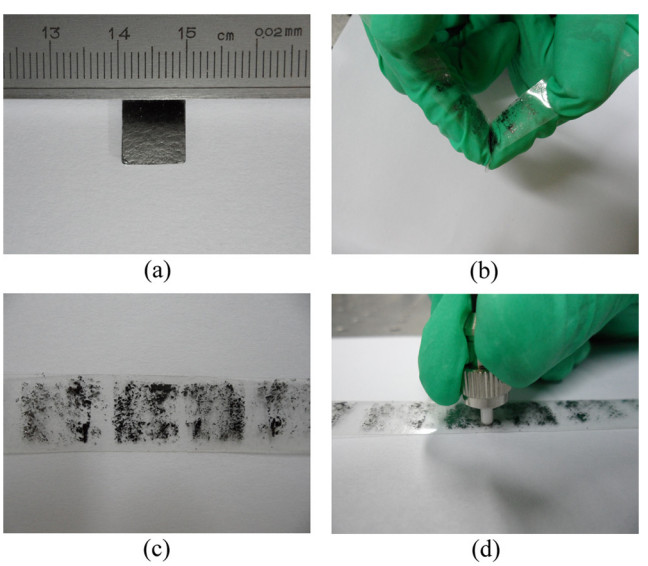

Fig. 1 Mechanical exfoliation of HOPG, (a) HOPG; (b) exfoliation of HOPG by scotch tape; (c) as-fabricated multilayer graphene sheets; and (d) deposition on a standard FC/PC fiber connector.

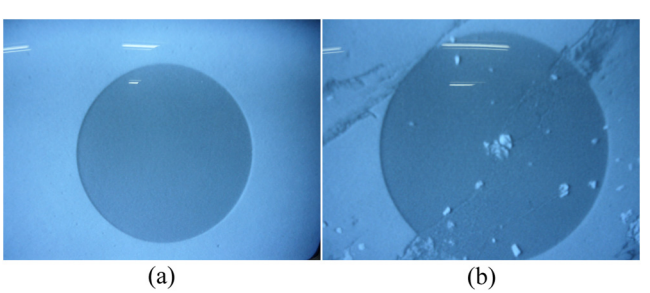

Fig. 2 The end facet of fiber ferrule (a) before contacting with graphene sheets and (b) after contacting with graphene sheets.

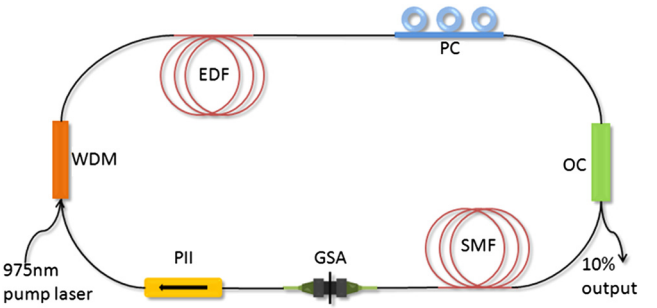

Fig. 3 Experimental setup of the GSA mode-locked fiber ring laser, erbium-doped fiber (EDF), standard single mode fiber (SMF), polarization controller (PC), output coupler (OC), polarization independent isolator (PII), wavelength-division multiplexer (WDM), and graphene-based saturable absorber (GSA).

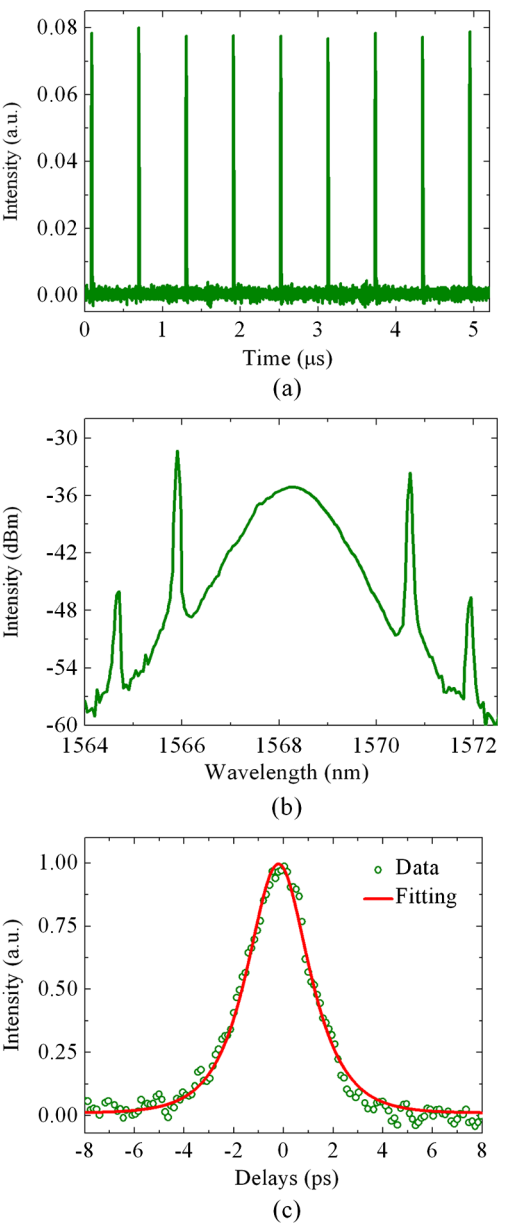

Fig. 4 (a) Oscilloscope trace; (b) optical spectrum; and (c) pulse autocorrelation trace of a typical single soliton operation.

graphene. It was afterward deposited on a standard FC/PC fiber connector just by pressing the ferrule onto the graphene-adherent side of the tape. Due to the adhesive Van der Waals force between the graphene film and SiO_2, multilayer graphene could be safely attached onto the end fiber facet as shown in Fig. 2.

In the following, another clean connector was used to connect as another side through a FC/PC adapter, constituting a graphene SA device, which could be spliced into the fiber laser cavity. The optical transmittance of the multilayer graphene is ~88% at 550 nm wavelength. This is corresponding to an average numbers of 5 graphene layers according to Nair et al.[34]

2.2 *Experimental Setup*

The graphene mode-locked fiber laser setup is schematically shown in Fig. 3.

The fiber laser has a ring cavity configuration, which comprises a piece of 1 m, high concentration erbium-doped fiber (EDF, LIEKKI Er80-8/125) with group velocity dispersion (GVD) of -20 ps^2/km at 1550 nm and a 105 m standard single mode fiber (SMF) with GVD of -23 ps^2/km. The total cavity length is about 117 m. The net cavity dispersion is about -2.688 ps^2. A polarization controller (PC) was used to control the cavity birefringence and a 10% output coupler (OC) was used to extract the cavity light. A polarization independent isolator (PII) was spliced to force the unidirectional operation of the ring cavity. And the laser cavity was pumped by a 975 nm laser diode (LD) with a maximum pumping power of 500 mW through a 975/1550 nm wavelength-division multiplexer (WDM). The graphene-based SA (GSA) was placed between SMF and PII to mode lock the fiber laser. An optical spectrum analyzer (OSA, Ando AQ-6317B), a digital oscilloscope (Tektronix TDS3054B) and a commercial second harmonic autocorrelator were used to observe and analyze the laser performance.

3 Results and Discussions

3.1 *Single Soliton State*

In our experiments, the threshold pump power for continuous wave (CW) operation is 131.0 mW. Once the pump power exceeds 171.4 mW, the mode-locking operation can be obtained with an average output power of 0.67 mW, just by appropriately adjusting the orientation of PC. Figure 4 shows the oscilloscope traces, the optical spectrum, and the corresponding autocorrelation trace of a single soliton state, respectively.

As shown in Fig. 4(a), the fundamental repetition is about 1.646 MHz, corresponding to a cavity round-trip time of about 607.53 ns and a cavity length of 117 m. Figure 4(b) shows the optical spectrum centered at 1568.3 nm and a 3 dB spectral width of about 1.61 nm. Figure 4(c) shows the autocorrelation trace with a full width at half maximum (FWHM) of about 2.92 ps. If the pulse profile is assuming to be sech^2 profile, the pulse duration is about 1.656 ps, which gives the time-bandwidth product of 0.325 and indicates that the mode-locked pulse is nearly transform limited.

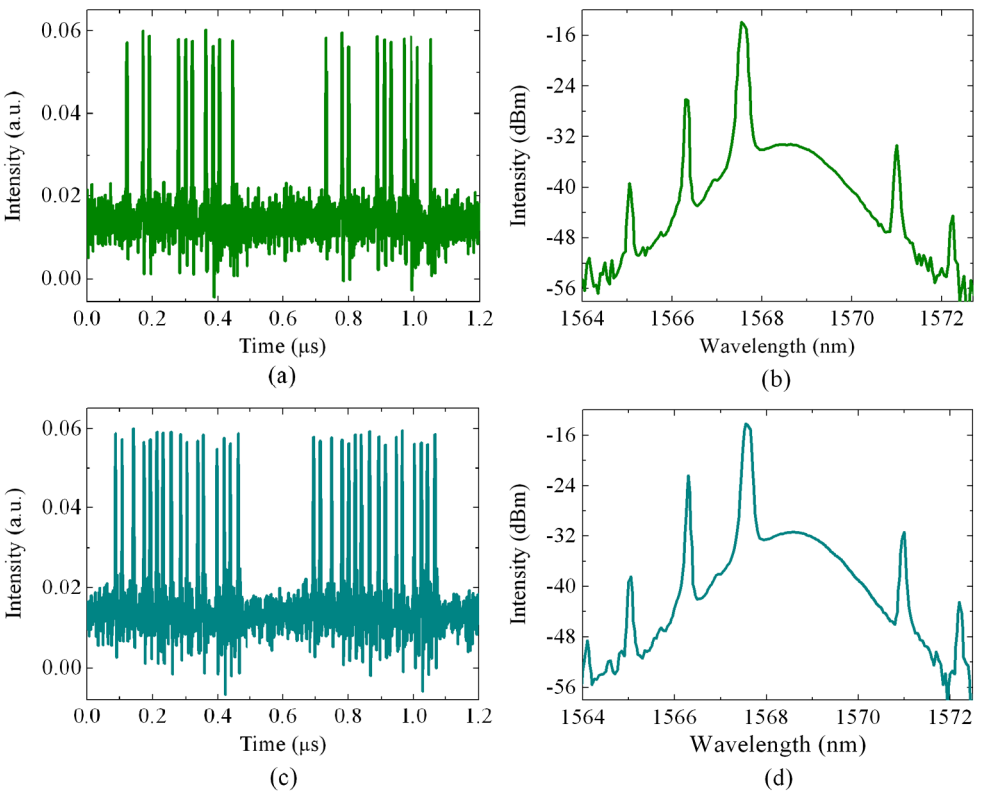

Fig. 5 (a) Ten soliton pulses coexist in a repetition period at a pump power of 178.3 mW and (b) its optical spectrum; (c) sixteen soliton pulses coexist in a repetition period at a pump power of 183.0 mW, and (d) its corresponding optical spectrum.

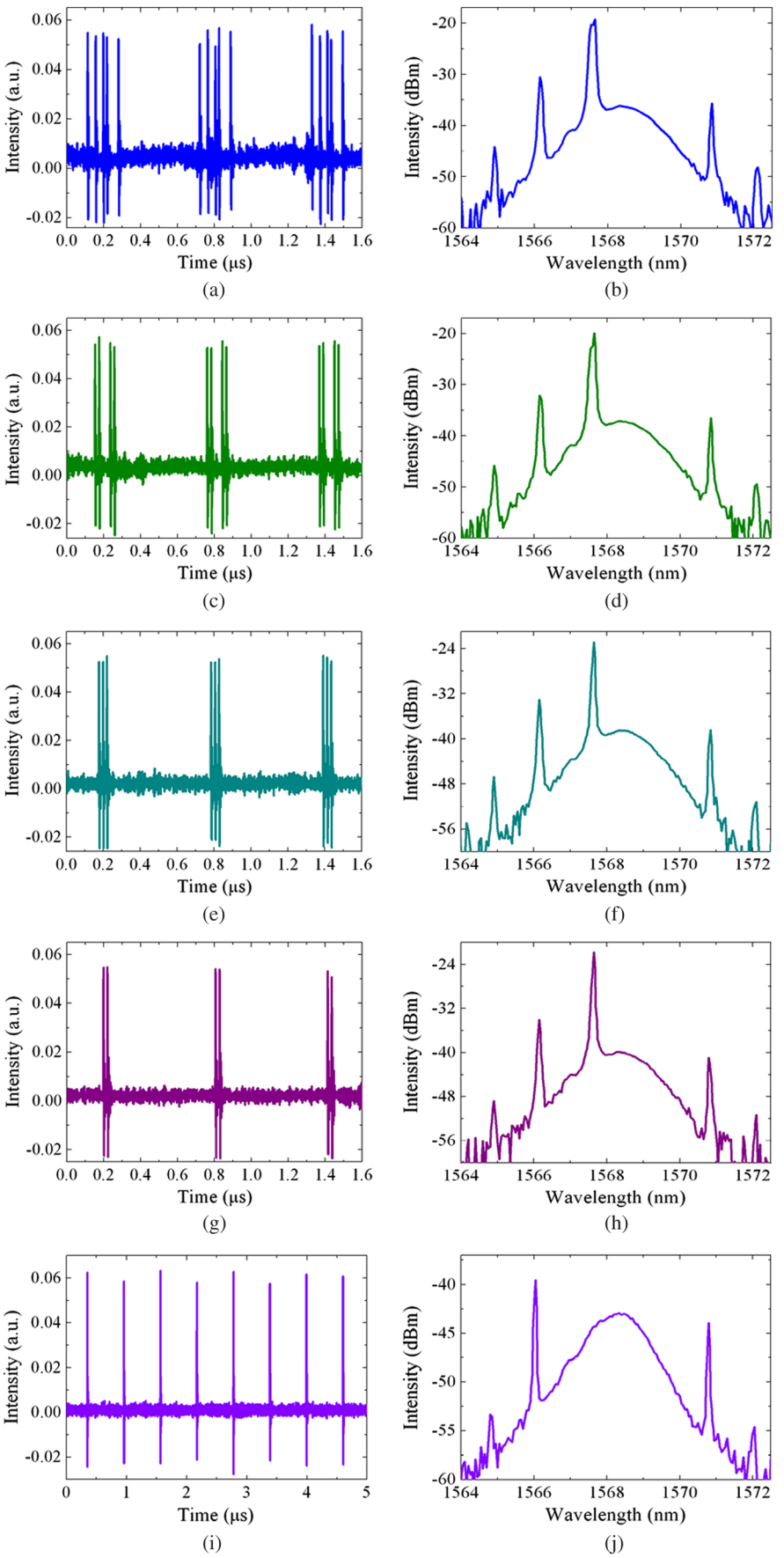

Fig. 6 (a) (c) (e) (g) (i) Annihilation of multisoliton state with the decrease of the pump power and (b) (d) (f) (h) (j) their corresponding optical spectrum, respectively.

3.2 *Ordered Multisoliton State*

Owing to the peak power clamping effect,[35] multisoliton state can be obtained by further increasing the pump power. Within this steady state, all soliton pulses have exactly similar pulse quality due to the soliton energy quantization effect,[35,36] leading to a static ordered multisoliton state as a result of mutual repulsion forces. They are grouped together but temporally separated, as shown in Fig. 5, under a pump power of 178.3 and 183.0 mW, respectively.

Besides the phenomena of the appearance of addition soliton pulse one by one through increasing the pump power, an inversed process: soliton annihilation was also experimentally observed by slightly decreasing the pump power. Starting from the multisoliton state in Fig. 6(a), soliton disappeared one by one, in which the number of solitons decreased from five to two, corresponding to a pump power of 120.4 mW, 112.4 mW, 101.3 mW, and 100.2 mW, respectively. Eventually, single soliton operation state was obtained at a pump power of 92.7 mW.

3.3 *Chaotic Multisoliton State*

With a further increase in the pump power, the ordered multisoliton state becomes unstable and a chaotic multisoliton state emerges. Under this state, the temporal distribution becomes relatively random. Both the partially random and completely random distribution of the chaotic multisoliton states are shown in Fig. 7.

The coexistence of CW and nonlinear wave components was seen in the spectrum. Two sets of spectral sidebands appear in the case of completely random distribution multisoliton state, indicating that CW component has already been shaped to nonlinear wave and symmetric spectral sidebands located around 1567 nm appear due to the resonant periodic constructive interference between the nonlinear dispersive wave and soliton component centered at 1567 nm. However, as the formed new solitons at 1567 nm has very weak pulse intensity, the mutual soliton interaction forces were very weak, indicating that the temporal locking between multisolitons failed. This accounts for why chaotic multisoliton pulses are completely random in temporal domain.

3.4 *Bunched Multisoliton State*

Bunched-soliton state, a group of soliton pulses temporally localized within a tight packet, could also be obtained, as shown in Fig. 8(a). We noted that under different pump powers, the bunched soliton state displays different pattern structures. The soliton bunch could exist stably in the cavity with the fundamental cavity repetition rate. Because the state is sensitive to the variation of the experiment conditions and the environment perturbations, one could easily observe another soliton bunch state in Fig. 8(c), where the formed bunches coexist with other solitons in the cavity with the pump power of 214.9 mW. Further increasing the pump power to 356.3 mW, we firstly observed another new state, where many different soliton bunches coexist and they move with a constant speed with respect to each other. This state is illustrated in Fig. 8(e) with an output of 2.747 mW.

3.5 *Harmonic Multisoliton State*

Harmonic mode locking is an important tool for high repetition rate pulse formation. To achieve a relatively stable harmonic mode locking state, the CW component inside

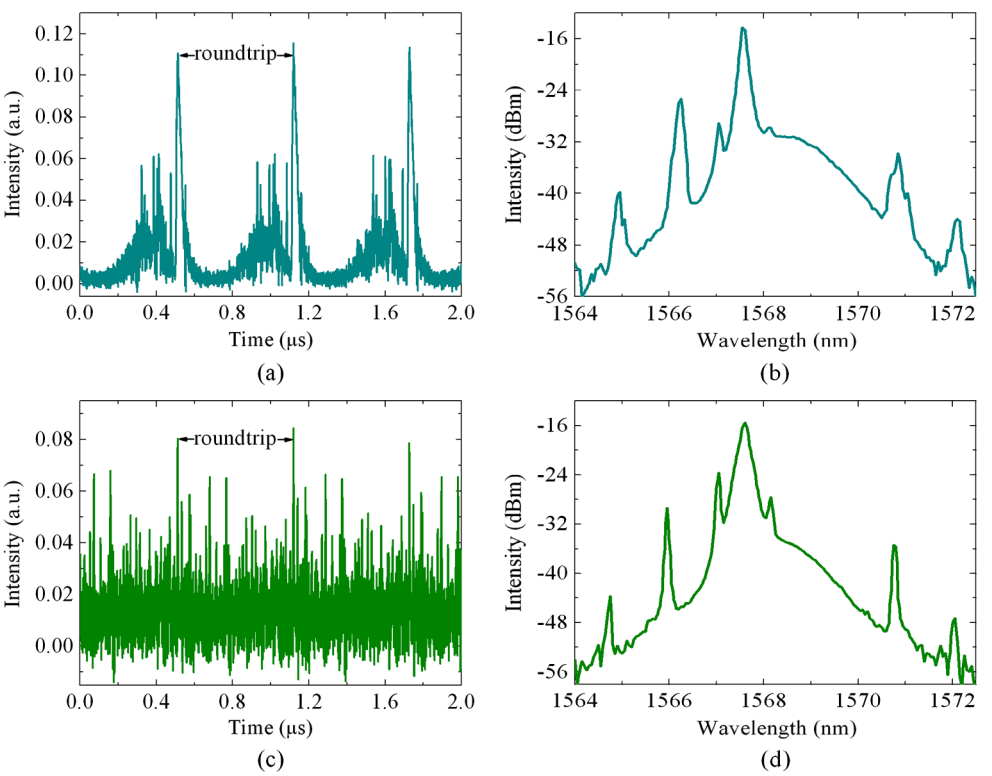

Fig. 7 (a) Partial-randomized distribution of chaotic multisoliton state and (b) its optical spectrum, and (c) complete-randomized distribution of chaotic multisoliton state, and (d) its corresponding optical spectrum.

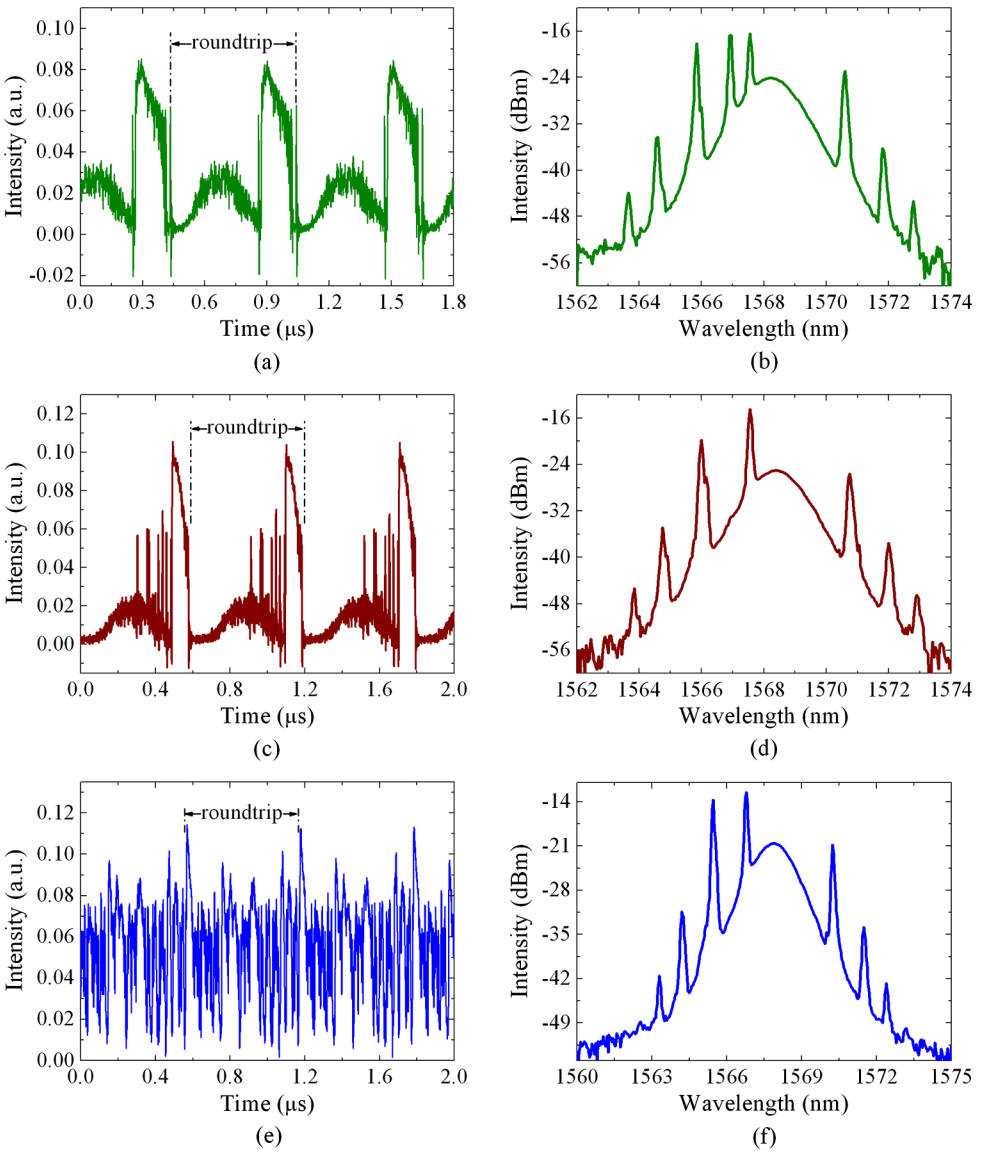

Fig. 8 (a) Soliton bunching with many soliton and (b) its optical spectrum; (c) soliton bunching coexists with other solitons and (d) its optical spectrum; (e) the coexistance of many soliton bunchings, and (f) its corresponding optical spectrum.

the laser cavity must be suppressed at a sufficiently weak level. As the CW lasing is intrinsically unstable in the laser due to the modulation instability, it eventually becomes unstable with the increasing pump strength. And this unstable CW lasing could introduce a kind of global soliton interaction among the adjacent solitons.[37] Therefore, by changing the pump power or the orientation of PC, the strength of the modulation instability (the unstable CW lasing) can be controlled. When the CW lasing is adjusted appropriately, the phases of all the solitons in the laser cavity could become synchronized to those of the CW lasing, and phase locking among them occurs,[26] leading to the formation of harmonic mode-locking (HML).

Starting from the multisoliton states in Fig. 9, in which, a cluster of optical soliton pulses randomly coexist together but separate in temporal domain, one can achieve the state of harmonic multisoliton operation state, as shown in Fig. 10, by slightly lowering the pump strength and rotating the orientation of the PCs. In our experiment, HML at 24.7 and 60.9 MHz was observed, corresponding to 15th and 37th harmonic of the fundamental cavity repetition rate, respectively. Figure 10(a) and 10(b) shows the oscillation trace and the optical spectrum of the 15th harmonic obtained at the pump power of 262.3 mW. Further increasing the pump power, one can obtain the 37th HML shown in Fig. 10(c) and 10(d) with the pump power of 344.6 mW.

In order to illustrate the relation between the pump power and different soliton states, Fig. 11 gives the profile of output power referred to input power. It indicates that single soliton state, ordered and disordered multisoliton states appeared under lower pump power; however, bunched multisoliton and harmonic multisoliton states appeared under relative strong pump power. This may give some guidance to further experimental study.

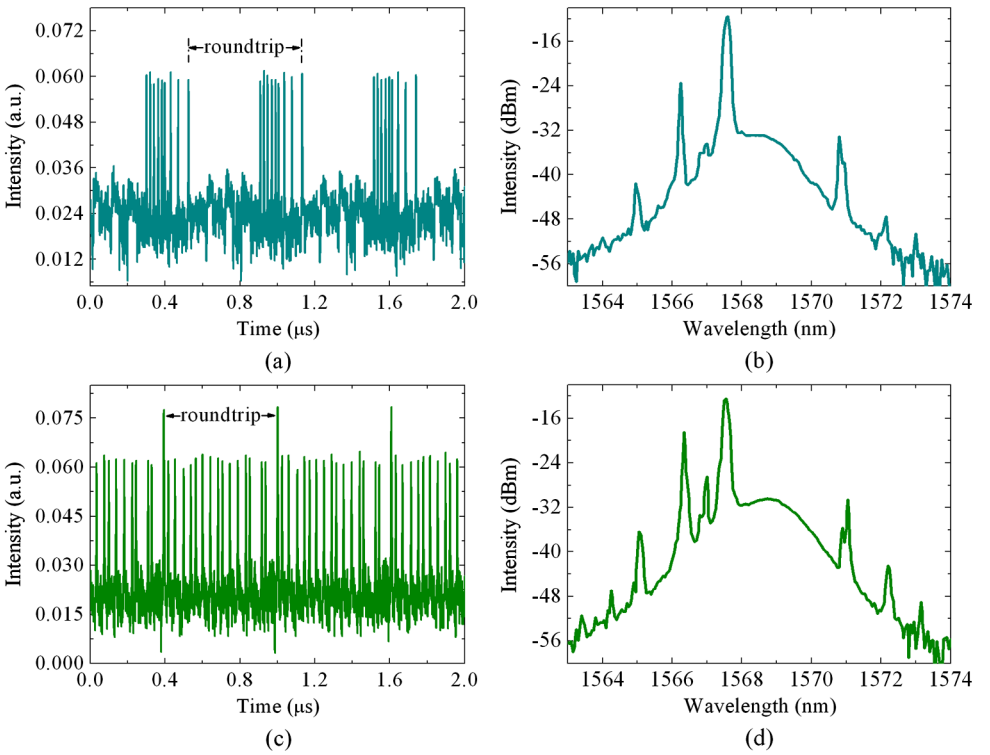

Fig. 9 (a) and (c) A cluster of soliton pulses compressed inside the laser cavity and (b) and (d) their corresponding optical spectrum, respectively.

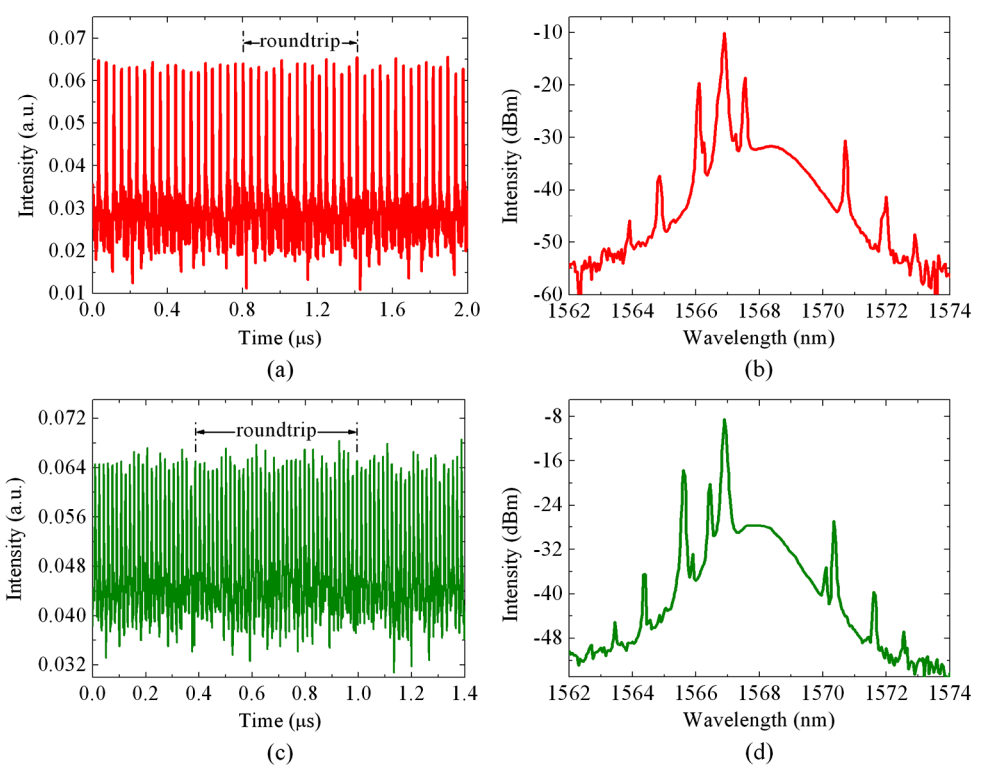

Fig. 10 (a) and (c) The 15th and 37th harmonic mode-locking state and (b) and (d) their corresponding optical spectrum, respectively.

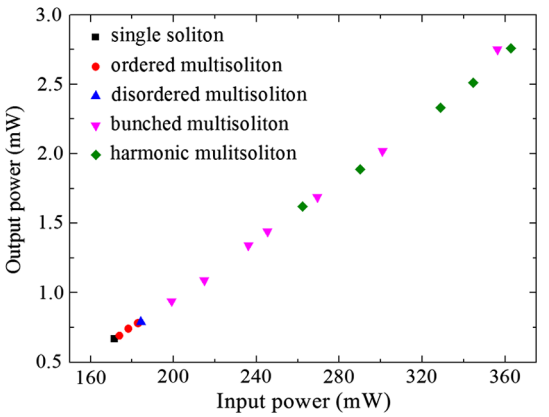

Fig. 11 The relation between pump power and different soliton states.

4 Conclusions

In conclusion, we systematically investigated the different soliton operation state in an erbium-doped fiber laser passively mode-locked graphene SA, fabricated by the mechanical exfoliation of HOPG. The laser cavity shows different operation states, including single-soliton, ordered-, chaotic-, and bunched-, and harmonic-multisoliton. This study shows that graphene could operate as a nonlinear optics element for soliton pattern formation in a graphene mode locking fiber laser, from which more interesting nonlinear optics dynamics could be expected in the future.

Acknowledgments

This work is supported by the Key Project of Natural Science Foundation of Hunan province (Grant No. 10JJ2047) and the Fundamental Research Funds for the Central Universities.

References

1. K. S. Novoselov et al., "Electric field effect in atomically thin carbon films," *Science* **306**(5696), 666–669 (2004).
2. Q. L. Bao et al., "Atomic layer graphene as saturable absorber for ultrafast pulsed lasers," *Adv. Funct. Mater.* **19**(19), 3077–3083 (2009).
3. H. Zhang et al., "Graphene mode locked, wavelength-tunable, dissipative soliton fiber laser," *Appl. Phys. Lett.* **96**(11), 111112 (2010).
4. Z. C. Luo et al., "Optical deposition of graphene saturable absorber integrated in a fiber laser using a slot collimator for passive mode-locking," *Appl. Phys. Express* **5**(5), 055103 (2012).
5. Z. W. Wang et al., "Switchable dual-wavelength synchronously Q-switched erbium-doped fiber laser based on graphene saturable absorber," *IEEE. Photon. J.* **4**(3), 869–876 (2012).
6. H. Zhang et al., "Large energy soliton erbium-doped fiber laser with a graphene-polymer composite mode locker," *Appl. Phys. Lett.* **95**(14), 141103 (2009).
7. H. Zhang et al., "Large energy mode locking of an erbium-doped fiber laser with atomic layer graphene," *Opt. Express* **17**(20), 17630–17635 (2009).
8. W. J. Cao et al., "Graphene-based, 50 nm wide-band tunable passively *Q*-switched fiber laser," *Laser Phys. Lett.* **9**(1), 54–58 (2012).
9. H. Zhang et al., "Compact graphene mode-locked wavelength-tunable erbium-doped fiber lasers: from all anomalous dispersion to all normal dispersion," *Laser Phys. Lett.* **7**(8), 591–596 (2010).
10. J. Sotor, G. Sobon, and K. M. Abramski, "Scalar soliton generation in all-polarization-maintaining, graphene mode-locked fiber laser," *Opt. Lett.* **37**(11), 2166–2168 (2012).
11. P. Huang et al., "Stable mode-locked fiber laser based on CVD fabricated graphene saturable absorber," *Opt. Express* **20**(3), 2460–2465 (2012).
12. Y. Chen et al., "Erbium-doped fiber laser passively mode-locked by a position-adjustable graphene saturable absorber," *Opt. Eng.* **51**(8), 084203 (2012).
13. Z. Q. Luo et al., "Multiwavelength mode-locked erbium-doped fiber laser based on the interaction of graphene and fiber-taper evanescent field," *Laser Phys. Lett.* **9**(3), 229–233 (2012).
14. Z. Liu, X. He, and D. N. Wang, "Passively mode-locked fiber laser based on a hollow-core photonic crystal fiber filled with few-layered graphene oxide solution," *Opt. Lett.* **36**(16), 3024–3026 (2011).
15. L. M. Zhao et al., "Dissipative soliton operation of an ytterbium-doped fiber laser mode locked with atomic multilayer graphene," *Opt. Lett.* **35**(21), 3622–3624 (2010).
16. Z. Luo et al., "Multiwavelength dissipative-soliton generation in Yb-fiber laser using graphene-deposited fiber-taper," *Photon. Technol. Lett.* **24**(17), 1539–1542 (2012).
17. J. Liu et al., "Passively mode-locked and Q-switched Yb-doped fiber lasers with graphene-based saturable absorber," *Chin. J. Lasers* **38**(8), 0802001 (2011).
18. J. Liu, Q. Wang, and P. Wang, "Graphene-based passively Q-switched 2 μm thulium-doped fiber laser," *Opt. Commun.* **285**(24), 5319–5322 (2012).
19. M. Zhang et al., "Tm-doped fiber laser mode-locked by graphene-polymer composite," *Opt. Express* **20**(22), 25077–25084 (2012).
20. W. D. Tan et al., "Mode locking of ceramic Nd: ytterbium aluminum garnet with graphene as a saturable absorber," *Appl. Phys. Lett.* **96**(3), 031106 (2010).
21. J. Xu et al., "Graphene saturable absorber mirror for ultra-fast-pulse solid-state laser," *Opt. Lett.* **36**(10), 1948–1950 (2011).
22. J. Xu et al., "Performance of large-area few-layer graphene saturable absorber in femtosecond bulk laser," *Appl. Phys. Lett.* **99**(26), 261107 (2011).
23. J. Ma et al., "Graphene mode-locked femtosecond laser at 2 μm wavelength," *Opt. Lett.* **37**(11), 2085–2087 (2012).
24. E. Hendry et al., "Coherent nonlinear optical response of graphene," *Phys. Rev. Lett.* **105**(9), 097401 (2010).
25. H. Zhang et al., "Z-scan measurement of the nonlinear refractive index of graphene," *Opt. Lett.* **37**(11), 1856–1858 (2012).
26. Y. Meng et al., "Multiple-soliton dynamic patterns in a graphene mode-locked fiber laser," *Opt. Express* **20**(6), 6685–6692 (2012).
27. G. Sobon, J. Sotor, and K. M. Abramski, "Passive harmonic mode-locking in Er-doped fiber laser based on graphene saturable absorber with repetition rates scalable to 2.22 GHz," *Appl. Phys. Lett.* **100**(16), 161109 (2012).
28. B. Fu et al., "Passive harmonic mode-locking in erbium-doped fiber laser with graphene saturable absorber," *Opt. Commun.* **286**, 304–308 (2013).
29. A. Reina et al., "Large area, few-layer graphene films on arbitrary substrates by chemical vapor deposition," *Nano Lett.* **9**(1), 30–35 (2009).
30. P. W. Sutter, J.-I. Flege, and E. A. Sutter, "Epitaxial graphene on ruthenium," *Nat. Mater.* **7**(5), 406–411 (2008).
31. S. Stankovich et al., "Synthesis of graphene-based nanosheets via chemical reduction of exfoliated graphite oxide," *Carbon* **45**(7), 1558–1565 (2007).
32. Y. M. Chang et al., "Multilayered graphene efficiently formed by mechanical exfoliation for nonlinear saturable absorbers in fiber mode-locked lasers," *Appl. Phys. Lett.* **97**(21), 211102 (2010).
33. J. Sotor et al., "Fundamental and harmonic mode-locking in erbium-doped fiber laser based on graphene saturable absorber," *Opt. Commun.* **285**(14), 3174–3178 (2012).
34. R. R. Nair et al., "Fine structure constant defines visual transparency of graphene," *Science*, **320**(5881), 1308 (2008).
35. D. Y. Tang et al., "Mechanism of multisoliton formation and soliton energy quantization in passively mode-locked fiber lasers," *Phys. Rev. A* **72**(4), 043816 (2005).
36. A. B. Grudinin, D. J. Richardson, and D. N. Payne, "Energy quantization in figure eight fiber laser," *Electron. Lett.* **28**(1), 67–68 (1992).
37. B. Zhao et al., "Passive harmonic mode locking of twin-pulse solitons in an erbium-doped fiber ring laser," *Opt. Commun.* **229**(4), 363–370 (2004).

Biographies and photographs of the author are not available.